NASA TECHNICAL TRANSLATION NASA TT F-16,114

ELECTRICAL CONDUCTIVITY OF THE POLAR IONOSPHERE

L.L. Van'yan and I.L. Osipova

Translation of "Elektroprovodnost' polyarnoy ionosfery," Academy of Sciences USSR, Institute of Space Research, Moscow, Report Pr-138, 1974, pp. 1-51

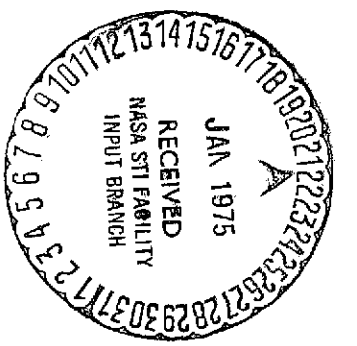

NATIONAL AERONAUTICS AND SPACE ADMINISTRATION
WASHINGTON, D.C. 20546 JANUARY 1975

STANDARD TITLE PAGE

1. Report No. NASA TT F-16,114	2. Government Accession No.	3. Recipient's Catalog No.
4. Title and Subtitle ELECTRICAL CONDUCTIVITY OF THE POLAR IONOSPHERE		5. Report Date January 1975 6. Performing Organization Code
7. Author(s) L. L. Van'yan and I. L. Osipova		8. Performing Organization Report No. 10. Work Unit No.
9. Performing Organization Name and Address Leo Kanner Associates Redwood City, California 94063		11. Contract or Grant No. NASw-2481 13. Type of Report and Period Covered Translation
12. Sponsoring Agency Name and Address National Aeronautics and Space Administration, Washington, D.C. 20546		14. Sponsoring Agency Code

15. Supplementary Notes

Translation of "Elektroprovodnost' polyarnoy ionosfery," Academy of Sciences USSR, Institute of Space Research, Moscow, Report: Pr-138, 1974, pp. 1-51

16. Abstract A study was made of the electrical conductivity of the polar ionosphere. The Hall and Pedersen conductivities of the sunlit and dark polar ionosphere were calculated from N(h)-profiles obtained from rocket measurements of electron concentrations and ground-based ionospheric probes. Integrated conductivities were obtained for the sunlit and dark polar ionosphere as functions of the maximum electron concentration of the E-layer, and also as functions of the activity of the horizontal component of the magnetic field. The conductivity of the auroral zone rises with increase in magnetic activity, but for $|\Delta T| > 250\ \gamma$ this increase in conductivity slows down. Plots of the electrical conductivity of the polar ionosphere were drawn for January, June, and September 1960 from measurements of the critical frequencies of the E-layer at the network of ionospheric stations, using the functions established.

17. Key Words (Selected by Author(s))	18. Distribution Statement		
	Unclassified - Unlimited		
19. Security Classif. (of this report) Unclassified	20. Security Classif. (of this page) Unclassified	21. No. of Pages	22. Price

NASA-HQ

INTRODUCTION

/3*

Analysis of electromagnetic fields in the polar ionosphere is impossible without detailed information on its electrical conductivity. Though enormous literature deals with this problem [1-97], nonetheless data on the geographical distribution of electrical conductivity are clearly inadequate. Electrical conductivity of the polar ionosphere depends on two factors: photoionization by solar radiation and ionization by fluxes of precipitating particles. As we know, three main zones can be differentiated by the nature of the precipitating particles in the polar ionosphere:

1. auroral zone,
2. region of daytime dip, and
3. polar cap.

The aim of this study is as follows: 1) analysis of electrical conductivity induced by precipitating particles in all three zones, its interactions with electrical conductivity caused by photoionization; 2) establishing integrated conductivity of the E-layer and magnetic activity; and 3) constructing schemes for the spatial distribution of electrical conductivity.

---

* Numbers in the margin indicate pagination in the foreign text.

POLAR

ELECTRICAL CONDUCTIVITY OF THE IONOSPHERE

L. L. Van'yan and I. L. Osipova

1. Method of Calculation

The conductivity of the ionosphere for low frequencies was calculated based on the generally accepted formulas (in the International System of Units): specific Pedersen electrical conductivity:

$$\sigma_P = Ne^2\left[\frac{\nu_e}{m(\omega_e^2+\nu_e^2)} + \frac{\nu_{in}}{M(\omega_i^2+\nu_{in}^2)}\right],$$

and specific Hall conductivity: /4

$$\sigma_H = Ne^2\left[\frac{\omega_e}{m(\omega_e^2+\nu_e^2)} - \frac{\omega_i}{M(\omega_i^2+\nu_{in}^2)}\right],$$

where ω_e is the cyclotron /or gyro/ frequency of electrons,

ω_i is the cyclotron frequency of ions,

ν_e is the total frequency of collisions of electrons with neutral particles and ions,

ν_{in} is the frequency of collisions with neutral particles,

e is the charge on an electron,

m and M are the masses of electron and ion, respectively, and

N is number density of electrons.

Since we are considering the high latitudes, we will assume that the geomagnetic force lines are normal to the plane of the ionosphere, so that $\sigma_{xx} = \sigma_{yy} = \sigma_P$, $\sigma_{xy} = -\sigma_{yx} = \sigma_H$.

As we can see from the formulas, specific electrical conductivity is the product of electron number density by electrical conductivity corresponding to unit concentration. Therefore our problem will be divided into two stages:

1. Analysis of unit electrical conductivity.

2. Analysis of spatial distribution of N.

The Jacchia 1970 neutral atmosphere model was used in the calculation of unit electrical conductivity [10] with exospheric temperature T_∞ = 1100° K. In order to find how strongly the selection of model affects integrated conductivity, the integrated conductivity was calculated for 30 different N(h)-profiles obtained at the stations Thule and Narssarsuak, using neutral models with T_∞ - 800° K and T_∞ = 1500°, which corresponds to a 53° K change in the temperature of neutral particles /5 at the elevation 120 km, and 92° K at the elevation 130 km. The results of calculations are given in Table 1, from which it is clear that Hall conductivity in this case varies by an average of 7 percent, and Pedersen -- by 20 percent, which falls within the limits of precision of the experimental data used.

Now let us examine methods of calculating the collision frequencies ν_e and ν_{in}. The dependence of δ_P on ν_e is substantial for all altitudes below 100 km where conductivity is low, while above this altitude δ_P and δ_H depend weakly on ν_e. In this study, ν_e was calculated based on formulas given in [11]; the electron temperature was taken as equal to the neutral particle temperature. The frequency of ion-neutral collisions in the ionosphere ν_{in} is the most important parameter, which has been studied most poorly by the present time. Usually collisions of ions with neutral particles are viewed as interactions of elastic spheres without allowing for electrical forces [11-13]. We used the paper by Stubbe [14], who presents expressions for the frequencies of collisions of ions with neutral particles, taking into account electrical interactions of the polarization and charge-exchange types. Based on the neutral atmosphere [10] for T_∞ = 1100°K and the ionic composition according to [15] presented in Table 2, using Stubbe's formulas

TABLE 1

Station	Date	Local time	Σ_H $T_\infty = T = 800^\circ K$	Σ_H $T_\infty = T = 1500^\circ K$	Deviation %	Σ_ρ $T_\infty = T = 800^\circ K$	Σ_ρ $T_\infty = T = 1500^\circ K$	Deviation %
I	2	3	4	5	6	7	8	9
Thule	VI 1961	01	3.6	3.9	8.1	3.8	4.8	21.2
		02	3.5	3.9	8.6	4.0	4.9	21.4
		03	4.2	4.6	8.2	4.4	5.5	21.2
		04	5.7	6.2	7.5	5.4	6.6	20.6
		05	5.9	6.4	7.1	5.5	6.7	20.2
		06	6.7	7.2	7.3	6.1	7.5	19.1
		07	6.1	6.6	8.5	6.5	8.0	20.0
		08	8.1	8.8	7.5	7.5	9.2	19.7
		09	9.4	10.0	6.8	8.0	9.7	19.2
		10	10.1	10.6	4.6	8.2	10.0	19.3
		11	9.6	10.3	7.1	8.7	10.5	19.0
		12	10.7	11.4	6.2	8.3	10.0	19.0
		13	8.5	9.1	7.4	9.0	9.8	7.8
		14	7.7	8.3	8.2	7.4	9.0	19.8
		15	7.7	8.3	7.6	7.3	8.9	19.6
		16	8.3	8.8	6.6	7.0	8.5	19.3
		17	7.0	7.5	7.3	6.5	8.0	19.8
		18	6.6	7.1	7.2	5.9	7.2	20.0
		19	5.4	5.8	7.3	5.0	6.2	20.6
		20	4.8	5.2	7.5	4.6	5.7	21.2
		21	3.1	3.4	9.8	3.8	4.7	21.4
		22	3.5	3.8	8.6	3.8	4.7	21.1
		23	3.2	3.5	8.3	3.5	4.3	20.7
Narssar-suak	VI 1966	12	11.7	12.5	7.1	10.4	12.5	18.8
		14	7.1	7.9	10.5	9.2	11.2	19.8
		15	9.2	10.0	7.9	9.2	11.2	19.3
		16	8.4	9.1	7.8	8.2	10.0	19.5
		17	7.2	7.9	7.9	7.4	9.0	19.8
		18	6.3	6.8	7.6	6.1	7.5	20.4
		20	3.7	4.1	9.9	4.6	5.7	20.0
				Mean	7.0		Mean	19.6

TABLE 2

Altitude H km	Ionic comp. %					Neutral composition %			
	O_2^+	NO^+	O^+	H^+	He^+	N_2	O_2	O	He
1	2	3	4	5	6	7	8	9	10
100	10	90	-	-	-	77	18	5	-
120	10	90	-	-	-	71	12	17	-
150	30	60	10	-	-	64	8	31	-
170	22	58	20	-	-	55	6	39	-
200	13	37	50	-	-	45	4	51	-
250	7	4	89	-	-	40	4	56	-
300	-	-	100	-	-	20	-	80	-
350	-	-	95,5	0,7	3,8	14	-	84	2
425	-	-	94	1	5	7,5	-	88,5	4

the following expression was derived:

$$\nu_{in} = K \cdot 10^{-9} N_n,$$

where N_n is number density of neutral particles.

The coefficient K is virtually equal to 0.9 up to the altitude 170 km, and then increases, reaching 1.7 at the altitude 300 km and remains constant up to 400 km (Fig. 1). Changes in the ionic model do not appreciably affect its magnitude.

In calculating the cyclotron frequencies, the magnitude of the magnetic field was based on the data in [16] for each coordinate point. /6

The results of calculating the unit specific electrical conductivity and also ν_{in} are gien in Table 3.

As already indicated, the distribution of electron number density with altitude (N(h)-profiles) is of decisive significance for the calculation of conductivity.

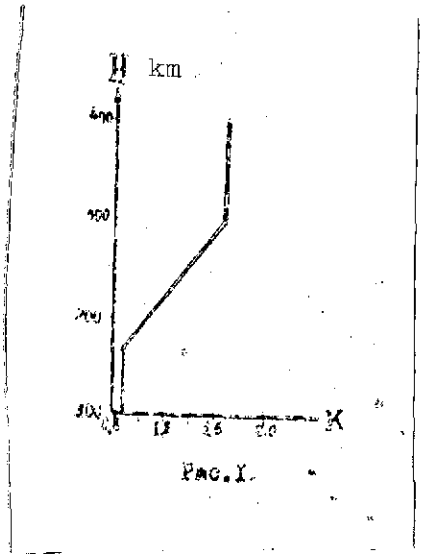

Fig. 1. Coefficient K as a function of altitude, H, km

In determining the integrated conductivity of the sunlit polar ionosphere, use was made of N(h)-profiles obtained from the data of ionic sounding at the stations Thule, Narssarsuak, and Godhavn. The following initial letters were used in calculating the nighttime integrated conductivity:

1. N(h)-profiles obtained from rocket measurements published in [6, 17-22]. Most of these characterize the nighttime auroral ionosphere for different geomagnetic conditions (Fig. 2 and Table 4).

2. The results of ground-based ionospheric soundings for moderate magnetic activity. In constructing the schemes of integrated conductivity of the ionosphere, use was made of the hourly values of f_oE. In those cases when f_oE was not determined, the value of f_BE_s of the sporadic layer with grouped delay can be used in calculating N. From Table 5 [21] it follows that the electronic number density calculated by f_BE_s agrees well with the results of rocket measurements at the E-layer maximum.

3. A comparison was made with ionization caused by fluxes measured on the Kosmos-261 satellite [23] and the integrated conductivity calculated on the basis of these data.

II. Regularities of Electrical Conductivity of Polar Ionosphere /7

1. Dark Polar Ionosphere

As already noted, at least three regions can be differentiated in the polar ionosphere: the auroral zone, the polar cap, and the

TABLE 3

№	H km	ν cm^{-1}	σ_T m^2/dm	σ_P m^2/dm
I	2	3	4	5
I	90	6.48×10^{4}	2.96×10^{-15}	1.18×10^{-16}
2	92	4.50	2.96	8.88×10^{-17}
3	94	3.14	2.96	7.10
4	96	2.17	2.96	6.24
5	98	1.51	2.96	6.23
6	100	1.05	2.96	7.08
7	102	7.25×10^{3}	2.96	8.90
8	104	5.15	2.96	1.17×10^{-16}
9	106	3.67	2.95	1.58
10	108	2.63	2.94	2.17
11	110	1.91	2.93	2.95
12	115	9.23×10^{2}	2.83	5.96
13	120	4.90	2.55	1.02×10^{-15}
14	125	2.85	1.99	1.39
15	130	1.80	1.31	1.47
16	135	1.22	7.79×10^{-16}	1.30
17	140	7.56×10^{1}	3.49	9.59×10^{-16}
18	145	6.41	2.54	8.29
19	150	4.92	1.51	6.52
20	155	3.87	9.39×10^{-17}	5.18
21	160	3.11	5.99	4.16
22	170	2.33	3.27	3.10
23	180	1.81	1.90	2.37
24	190	1.32	9.75×10^{-18}	1.70
25	200	1.08×10	6.21	1.35
26	210	8.21×10^{0}	3.45	1.01
27	220	6.87	2.33	8.3×10^{-17}
28	230	5.79	1.59	6.85
29	240	4.95	5.00×10^{-19}	5.33
30	250	3.93	4.19	4.48
31	260	3.37	4.64	3.79
32	270	3.21	4.22	3.53
33	280	2.37	2.24	2.58
34	290	1.95	1.46	2.00
35	300	1.61	–	1.69
36	310	1.33	–	1.39
37	320	1.21	–	1.24
38	330	0.93	–	9.43×10^{-18}
39	340	0.78	–	7.81
40	350	0.66	–	6.50
41	360	0.54	–	5.27
42	370	0.47	–	4.55
43	380	0.23	–	2.19
44	380	0.34	–	3.22

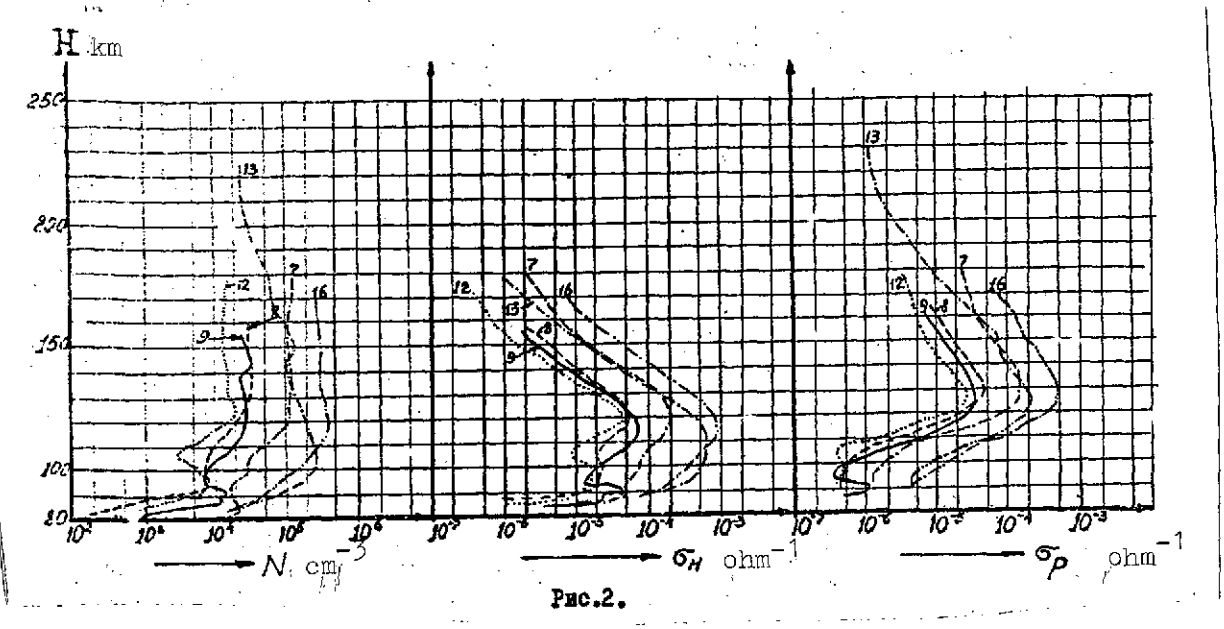

Рис.2.

Fig. 2. Altitude distribution of electron number density N, Pedersen conductivity Σ_p and Hall conductivity Σ_H in quiet and active geomagnetic conditions

daytime dip region. Let us examine the electrical conductivity of the ionosphere for each of these regions:

Auroral zone. The N(h)-profiles 9, 8, and 12 shown in Fig. 2 [21] characterize the electron number density in the auroral zone in magnetically-quiet conditions. These profiles have the following characteristics:

1. Ionization at the level of the E-layer reaches a value of approximately $3 \cdot 10^4$ cm^{-3}, which exceeds the number density in the middle-latitudinal night E-layer by approximately one order of magnitude. The precipitating of charged particles in the auroral zone sustaining the intensified ionization exists even in a magnetically-quiet period [21].

2. In the N(h)-profiles in the nighttime auroral zone there is no "valley" between the E- and F-layers usually

TABLE 4

Nr.	Observation site	Geog. coor. λ	Geog. coor. φ	Geomag. coor. Λ	Geomag. coor. Φ	Launch date	Time	Σ_H mho	Σ_P mho	Σ_H/Σ_P	ΔT_H γ	$N_{E max}$	References
1	Kiruna 67°50	20°25 E		+65°.3	115°.6	26.3.66.	20.05 LT	28.4	13.2	2	250	2.5.10^5	[20]
2						15.6.66.	01.14	19.4	6.5	3	Quiet	2.10^5	[20]
3	Church-58°48	94		+68°.7	322°.8	27.X.64.	circa 11.00 CST	6.7	-	-		0.65.10^5	[17]
4	Hill					13.3.65.	01.48	29	14	2	146	5.5.10^5	[18]
5						6.3.65.	01.30	14	10.2	1.3	88	2.10^5	[18]
6						15.9.66.	19.25	4.0	3.9	1	50	1.15.10^5	[21]
7						15.9.66.	21.00	6.2	5.0	1.2	70	1.05.10^5	[21]
8						13.9.66.	24.23	1.6	1.6	1.0	Quiet	0.28.10^5	[21]
9						13.9.66.	19.35	2.0	1.5	1.3	Quiet	0.21.10^5	[21]
10						31.X.64.	23.55	29	15	1.9	Act.	3.3.10^5	[21]
11						27.2.65.	18.21	5.3	3.8	1.4	50	0.85.10^5	[21]
12						5.X.65.	18.21	1.1	1.2	0.9	Quiet	0.2.10^5	[21]
13						8.2.64.	22.15	19.6	6.6	3	200	2.2.10^5	[22]
14	Kiruna67°50	20°25 E		+65°.3	115°.6	19.11.68	02.36 LT	28	12.2	2.3	170	3.2.10^5	[6]
15						4.12.68	23.26	33.5	15	2.2	240	3.3.10^5	[6]
16						3.12.68	22.59	24.6	14.3	1.7	300	3.1.10^5	[6]
17						30.11.66	night	41.3	-	-	-	5.1.10^5	[19]
18						29.11.66	night	24	-	-	-	3 .10^5	[19]
19	Church-58°48	94°06		+68°.7	322°.8	4.6.67.	12.16 CST	18	14	1.3	-	2 .10^5	[29]
20	Dumon-	66°40	140°00	-75°.	230°.8	8.1.67.	22.05 LT	1.0	0.6	1.6	-	0.11.10^5	[27]
21	Dorville					29.1.67.	11.20	20	16.5	1.2	-	2 .10^5	[27]

observed at night at the middle latitudes. Using the N(h)-profiles 8, 9, and 12, and the table of unit conductivity, the altitude profiles of Σ_H and Σ_P were calculated. It was found that Hall conductivity is substantial in the layer at altitudes from 100 to 140 km and has a maximum $(4.5\text{-}7.0)\cdot10^{-5}$ mho/m at the altitude 115-120 km. In the lower part of the profile there appear thin layers of intensified conductivity associated with the irregularities of electron number density. Pedersen conductivity drops off with altitude much more slowly: its maximum $(2.7\text{-}4.5)\cdot10^{-5}$ mho/m) occurs at the altitude 125-130 km (Fig. 2).

The integrated Hall conductivity is Σ_H = 1.1-2.0 mho, and /8
the integrated Pedersen conductivity Σ_P = 0.9-1.3 mho. It must be remembered that the N(h)-profiles used for the calculation are inadequately extensive and do not take into account the contribution made by the F-layer to the integrated Pedersen conductivity. To estimate the magnitude of this contribution, we used a typical N(h)-profile for the quiet nighttime high-latitude ionosphere /8/. The integrated Pedersen conductivity of the region of the ionosphere from 160 to 400 km calculated based on this profile is approximately 0.5 mho. In the estimates of the conductivity in this same range of altitudes based on the night N(h)-profiles for the Narssarsuak Station, the values of 0.3-0.5 cm^{-1} were obtained. Taking this correction into account, the Pedersen conductivity of the auroral zone in quiet conditions will be 1.2-1.6 cm^{-1}. For comparison, we point out that in the nighttime ionosphere at the geomagnetic latitude 50°, Σ_H = 0.4 mho and Σ_P = 0.3 mho /8/. Thus, even in magnetically-quiet conditions $\Sigma_{H,P}$ of the nighttime auroral ionosphere exceeds by three to four times the corresponding conductivities of the nighttime middle-latitude ionosphere. Similar results were obtained in /8/.

The electron number density in the E-layer of the ionosphere increases with rise in magnetic activity. Fig. 2 presents the electron number density profile 7, 13, and 16 for magnetically-active conditions, and the corresponding profiles of δ_H and δ_P. The magnitude of the horizontal component of the magnetic activity vector $|\Delta T_H|$ is given in Table 4. (The numbering of the curves in the table and in the figure is identical.) Analysis of all the profiles shown indicates that the nighttime auroral E-layer is similar in terms of the electron number density to the regular daytime E-layer and exceeds by more than one order the number density of the surrounding nighttime ionosphere, but its thickness as a rule is less than in the daytime ionosphere, and the shape of the profile changes from instance to instance as a function of the properties of the invading fluxes. /9

With increase in magnetic activity, the maximum of the Hall conductivity rises from 10^{-4} to 10^{-3} mho/m, while that of the Pedersen conductivity increases from 10^{-4} to $5 \cdot 10^{-4}$ mho/m. The integrated conductivity also increases, whose values are given in Table 4. Results of the calculations suggest conclusions concerning the ratio of Σ_H and Σ_P in the auroral zone. We know that this ratio is assumed to be very large in many papers. Thus, in [24] $\Sigma_H/\Sigma_P \sim 20$, in [25] $\Sigma_H/\Sigma_P \sim 13$, and in [26] -- -- $\sim 10^4$. Our calculations show that $\Sigma_H/\Sigma_P \sim 1$ in the quiet nighttime auroral zone. With increase in magnetic activity within these limits and the E-layer number density, this ratio rises, but does not exceed $\Sigma_H/\Sigma_P = 3$.

Since the main contribution to conductivity is made by the E-layer, it was of interest to establish a relationship between the integrated conductivities and the maximum electron number density of this layer. This function was plotted from 17 points (Table 4 and Fig. 3), where the coefficient of corre-

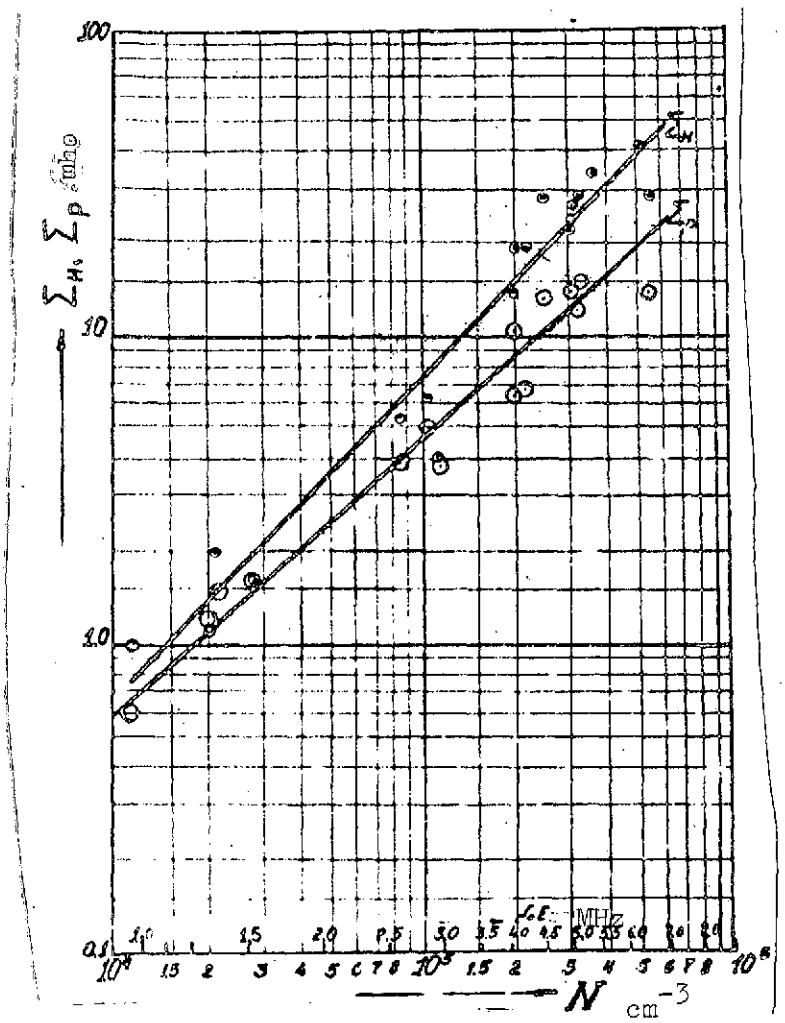

Fig. 3. Plot of the integrated Hall conductivity Σ_H and Pedersen conductivity Σ_P as functions of maximum concentration of E-layer for dark polar ionosphere

lation of was 0.9. The functions shown in bilogarithmic scale can be approximated by straight lines. The scatter on the average is 20 percent for the Hall conductivity and 15 percent for the Pedersen conductivity, although there are individual deviations up to 50 percent. The functions plotted enable us to estimate Σ_H and Σ_P of the auroral zone by using the critical frequencies of the E-layer based on data of ionic soundings. /10

It was of no less interest to establish how the conductivity changes in the function of the strength of the magnetic disturbance. This function was plotted for disturbances up to 180 γ in /9/.

Table 4 gives the data on the magnitudes of $|\Delta T_H| = \sqrt{\Delta x^2 + \Delta y^2}$ at the moments when Σ_H and Σ_P were calculated from rocket measurements. In addition, we can use the dependence of conductivity on the number density of the E-layer ($\Sigma_{H,P} = f(N)$),

or, which amounts to the same thing, as a function of the critical frequency of the E-layer ($\Sigma_{H,P} = f(f_oE)$), if we can find the correlation between f_oE and $|\Delta T_H|$. To do this, 37 measurements of f_oE and $|\Delta T_H|$ were compared at the stations Churchill, Point Barrow, Murmansk, Tiksi, and Dikson (Table 6). The coefficient of correlation is 0.8 (Fig. 4). The circles designate mean values, which quite satisfactorily fit on a straight line. The scatter of points is quite large, but the general tendency toward an increase in the critical frequency with an increase in $|\Delta T_H|$ shows up clearly. Using the function $\Sigma_{H,P} = f(N)$ (Fig. 3), from the critical frequencies of the E-layer we can convert to integrated conductivities. Using the data thus obtained and the results of the calculation from Table 4, Σ_H and Σ_P were plotted as functions of $|\Delta T_H|$. In Fig. 5, the crosses and points denote the values of Σ_H and Σ_P calculated from the rocket data, and the crosses and points within circles denote data calculated from averaged values of f_oE. In spite of the considerable scatter of the points, from the graph it is clear that with increase in the magnetic disturbance, conductivity rises, and its growth slows down for large $|\Delta T_H|$. /11/

Polar cap. The most sparce information is available on the nature of the ionization in the dark polar cap. Only one rocket measurement of the electron number density is described, on 20 January 1967 at the Antarctic station Dumon-Durville /27/ Fig. 6. The launch occurred under conditions of moderate magnetic activity (K = 5) and in conditions of increased solar activity (a scale 3 solar flare was observed in this day). The maximum concentration in the E-layer was $1.2 \cdot 10^4$ cm^3. The N(h)-profile suggests the N(h)-profiles in the quiet auroral zone, although the number densities are 1.5-2 times lower. The conductivities calculated by this profile are $\Sigma_P = 0.6$ mho and

TABLE 5

Nr.	Launch number	Date and time of launch	From rocket data: max. $\times 10^{+4}$ cm^{-3}	From rocket data: plasma frequency, MHz	f_0E_s MHz	f_0E_s MHz	Type E_s	Remark
1	2	3	4	5	6	7	8	9
1.	I4.I97	31.I0.I964 23.59.CST	33	5,I7	4,0	II,5	a	
2.	I4.I96	27.02.I965 I8.2I.CST	8,5	2,62	2,6	3,9	2	
3.	I4.202	5.I0.I965 I8.2I.CST	2,0	I,27	I,3	2,2	h end c & l	
4.	I4.278	I3.09.I966 I9.35.CST	2,6 (2,I)	I,45 (I,3)	I,6 (I,3)	2,8 (I,75)	2	for I40 km for I25 km
5.	I4.279	I3.09.I966 22.23.CST	2,8	I,5I	I,8	2,9	2	
6.	I4.280	I5.09.I966 I9.25 CST	II,5	3,05	2,8	5,6	2 & a	
7.	I4.28I	I5.09.I966 2I.00	I0,5	2,92	2,7	I2,0	a	

TABLE 6

Nr	Station	Date	Time	f_0E	$\lvert\Delta T_H\rvert$
I	Churchill	25.2.65	04^{00}	3.3	53
2		II.2.65	00^{30}	2.2	I03
3		20.2.65	00^{00}	2.0	25
4		I.4.60	02^{00}	5.5	270
5	Tiksi	I7.I.60	23^{00}	3.6	40
6			22^{30}	4.0	I20
7		25.I.60	02^{00}	5.2	200
8		I7.I.60	02^{00}	3.5	I00
9			03^{00}	3.9	I30
I0			07^{00}	2.3	70
II	Murmansk	I7.I.60	$I7^{00}$	2.0	54
I2		9.I.60	$2I^{00}$	5.I	I50
I3	Dikson	9.I.60	04^{00}	3.9	I20
I4			05^{00}	4.0	I40
I5		I7.I.60	$0I^{00}$	4.0	I85
I6			05^{00}	5.2	340
I7			$2I^{00}$	4.0	I80
I8		25.I.60	00	3.2	I05
I9		I.I.60	04^{00}	3.5	I60
20		25.I.60	04^{00}	4.3	I50
2I	Churchill	25.I.60	24^{00}	3.0	65
24			08^{00}	3.5	75
25		I.I.60	23^{00}	4.0	I60
26			00^{00}	I.8	70
27			08^{00}	3.2	80
28			05^{00}	2.7	60
29			$0I^{00}$	2.3	I00
30			02^{00}	2.2	50
3I		I7.I.60	00^{00}	6.8	330
32			$0I^{00}$	3.4	I09
33			02^{00}	2.3	40
34			03^{00}	3.4	75
35			07^{00}	4.2	II0
36			08^{00}	3.0	I00
37		27.2.65	20^{30}	3.0	I20

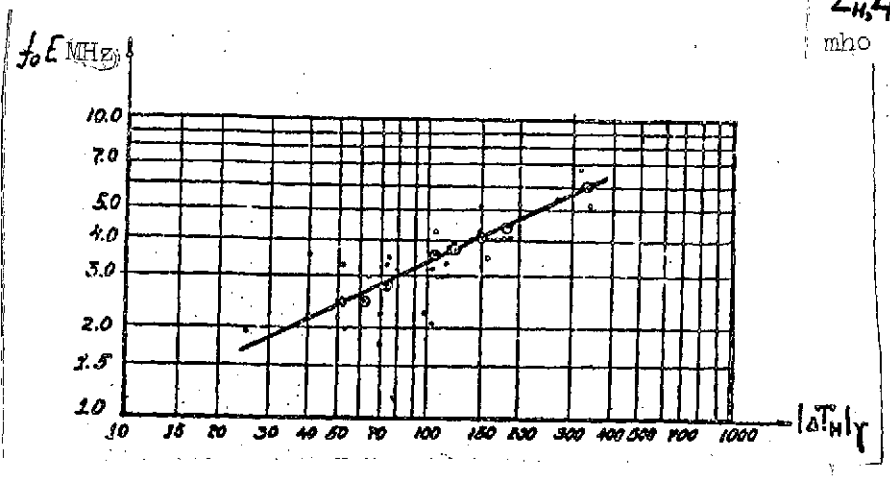

Fig. 4. Plot of critical frequency of E-layer (f_0 E) as a function of the horizontal vector of magnetic activity $|\Delta T_H|$

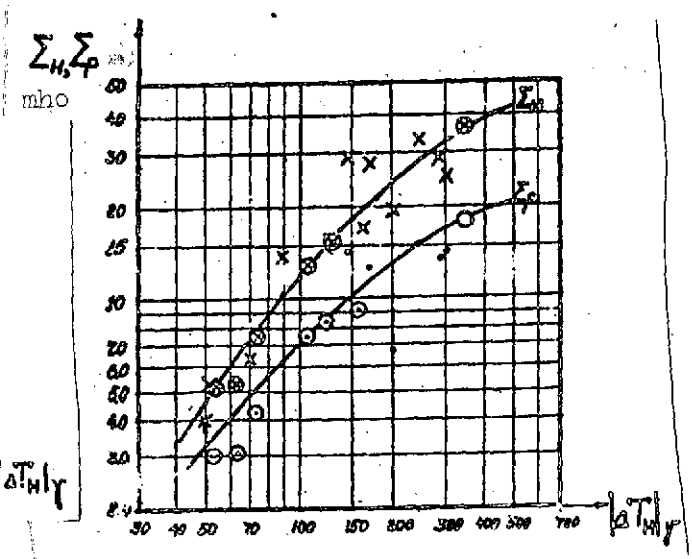

Fig. 5. Plot of integrated Hall conductivity Σ_H and Pedersen conductivity Σ_P as functions of the horizontal vector of magnetic activity $|\Delta T_H|$

Σ_H = 1.0 mho. These values agree closely with the plot of $\Sigma_{H,P} = f(N)$ for the dark auroral zone.

In December 1968, during the overflight of the Kosmos-261 satellite over the polar cap, fluxes of precipitating particles were measured. From these data, the ionization produced by the fluxes during a period of moderate magnetic activity was estimated and the conductivities were calculated: Σ_H = 1.1 mho and Σ_P = 0.55 mho [23]. This agrees well with the results of the rocket experiment at the station Dumon-Durville. Measurement of the critical frequencies of E-layer in the polar cap were difficult, since the measured quantity often proved to be lower than the lower limit of the working frequency of the

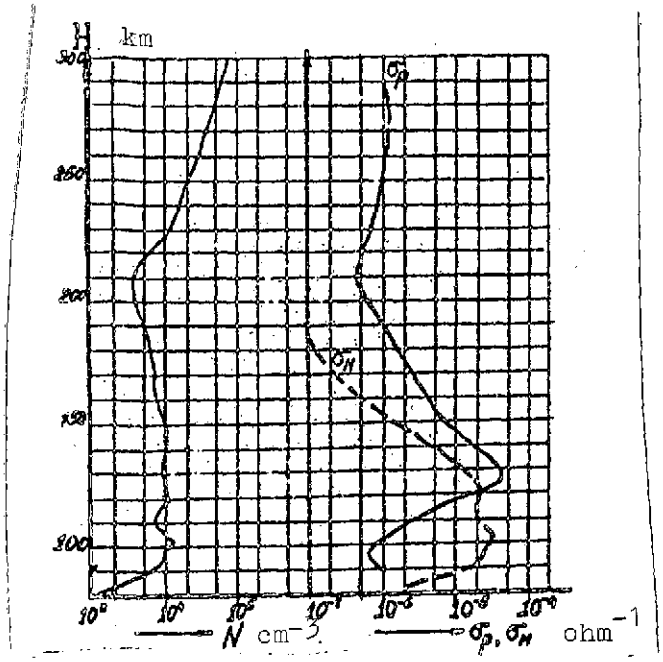

Fig. 6. Altitude distribution of electron concentration N, Pedersen conductivity Σ_P, and Hall conductivity Σ_H at Dumon-Durville Station

standard ionospheric stations, 1 MHz. This did not permit determining the limiting values of f_oE. O. P. Kolomiytsev, taking ovservations at the Vostok station in the Antarctic in the winter of 1958, indicated the existence /12 of a regular nighttime E-layer with a critical frequency of about 1 MHz, which corresponds to the concentration of the E-layer measured in the experiment at the station Dumon-Durville /28/ Analysis of the values of f_oE and f_BE_s for January over a period of several years at the Godhavn station showed that the nighttime values of these quantities fluctuates within the range 1.0-1.5 MHz, in a number of rare cases reaching 2 MHz (the lower limit was determined by the technical capabilities of the measurements). This corresponds to $\Sigma_P \sim 0.5 \cdot 1.2$ mho and $\Sigma_H \sim 0.8$-2 mho. All this indicates that the polar cap ionosphere is also subjected to conductivity fluctuations, but to a considerably lesser degree than the auroral zone.

Region of Daytime Dip (Geomagnetic Latitudes 78-81°)

There are even less data on the conductivity in this region in the dark conditions than for the polar cap. The estimate of the conductivity based on calculations of ionization caused by fluxes measured on the Kosmos-261 satellite /23/ give values

of Σ_P = 2 mho and Σ_H = 3 mho. Estimates of conductivity for the Godhavn station by analysis of January values of f_oE give $\Sigma_P \sim$ 2.5 mho and $\Sigma_H \sim$ 4.0 mho, which satisfactorily agree with the conductivities obtained from satellite data. This suggests that the integrated conductivity in this region is 2-4 times greater than the conductivity in the polar cap.

2. Sunlit Polar Ionosphere

To determine the conductivity of the sunlit polar ionosphere, we used 212 N(h)-profiles plotted from the results of ionic soundings at the stations Thule, Godhavn, and Narssarsuak in quiet geomagnetic conditions for different levels of sunlight and solar activity. /13

Daytime values of Σ_H and Σ_P vary approximately from 3 mho near the terminator to 13 mho at the zenith angle of the Sun $\chi \approx 40^\circ$. The relationship between the magnitudes of the daytime integrated conductivities and the electron number density at the maximum of the E-layer shown in Fig. 7 is clearly visible. The points denoted with circles refer to the arithmetic mean conductivities obtained from 4-28 measurements. In the graph are shown also the maximum deviation from the main. The linear dependence of $\lg \Sigma_{H,P}$ on $\lg N$ is well defined. The values of the mean and maximum scatter of the calculated values of Σ_H and Σ_P are given in Table 7. The mean scatter of the values does not exceed 20 percent; there are only individual jumps with a maximum deviation up to 50 percent. Calculations show that Σ_H / Σ_P is close to unity (Fig. 8). It is somewhat less than unity in the morning and evening hours and somewhat greater around noontime.

The correctness of these correlations can be checked by two rocket measurements made at the station Churchill on 4 June 1957 at 11:16, CST /29/ and the station Dumon-Durville on 29 January 1967 at 11:20 LT /local time/ /27/.

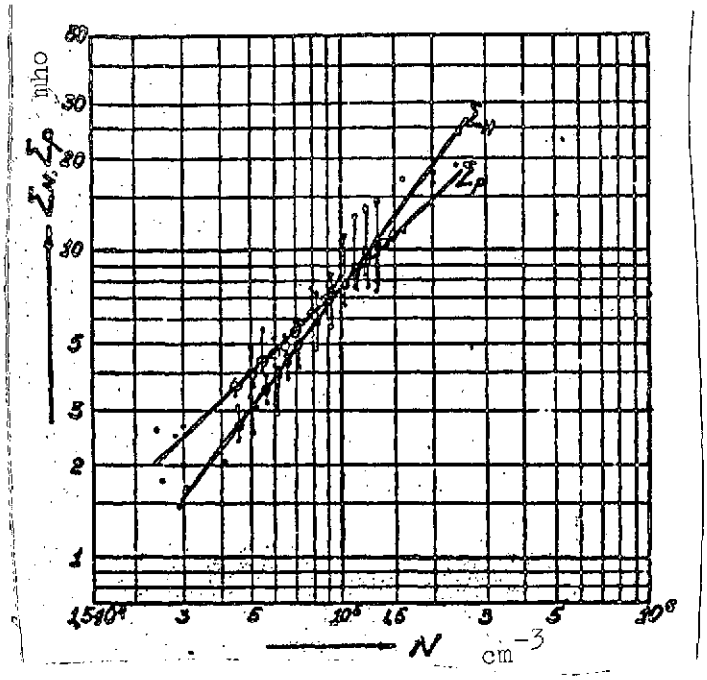

Fig. 7. Integrated Hall and integrated Pederson conductivities as functions of maximum concentration of E-layer for sunlit polar ionosphere

In both cases the measurements were taken under conditions of high solar activity and solar zenith angle ($\chi \approx 45^\circ$). The results of the measurements are as follows: at the station Churchill Σ_H = 18 mho, Σ_P = 14 mho, Σ_H/Σ_P = 1.3 mho; at the station Dumon-Durville Σ_H = 20 mho, Σ_P = 16.5 mho, and Σ_H/Σ_P = 1.2 mho.

In both cases the results agree well with /14 with the statistical dependence $\Sigma_{H,P} = f(N)$ for the sunlit polar ionosphere. Ionization of the ionosphere associated with the wave radiation of the Sun is evidently primary in the sunlit polar ionosphere in quiet geomagnetic conditions. The dependence of conductivities on the solar zenith angle χ is very satisfactorily approximated by the sine law:

$$\Sigma_P = 13\cos^{0.7}\chi,$$
$$\Sigma_H = 14\cos^{0.88}\chi.$$

Thus, ionization by flux in the polar cap and the region of the daytime dip is several times weaker than ionization by solar radiation, especially when the angle χ is close to 45°. The same can be said also concerning the auroral zone in magnetically-quiet conditions. During the periods of magnetic activity, ionization of the auroral zone associated with fluxes increases

TABLE 7

Nr	N cm^{-3} at maximum of E-layer	Mean value		Mean deviation from mean value		Maximum dev. from mean value	
		Σ_H mho	Σ_P mho	$\Delta\Sigma_H$ %	$\Delta\Sigma_P$ %	Σ_H %	Σ_P %
I	2	3	4	5	6	7	8
I.	$4.5 \cdot 10^4$	2,7	3,6	8,I	3,3	I8	50
2.	5,0	3,I	3,9	II,6	5,8	4I,9	20,5
3.	5,5	3,6	4,4	4,9	7,6	II,I	7,0
4.	6,0	3,9	4,6	I3,I	4,3	25,7	9,7
5.	6,5	4,3	4,9	6,2	3,2	II,6	8,2
6.	7,0	5,0	5,4	7,4	3,0	I8,0	4,5
7.	8,0	5,9	6,2	8,8	7,2	27,I	22,6
8.	9,0	6,9	6,8	I4,5	4,0	27,5	I6,2
9.	9,5	7,I	7,I	I3,I	2,5	36,6	5,6
I0.	$I0 \times I0^5$	7,9	7,7	I3,6	3,8	43,0	9,I
II.	I,I	8,8	8,3	I5,2	3,7	47,7	I0,8
I2.	I,2	9,6	9,I	I3,5	2,8	46,8	II,2
I3.	I,3	I0,5	9,8	I8,4	4,I	4I,2	2I,4

and can make a substantial contribution to total conductivity equal to or greater than the contribution made by photoionization.

Reliability of Results

Above we already presented data on the deviation from the mean values in the plotting of the empirical functions $\Sigma_{H,P} = f(N)$ for the sunlit and dark ionosphere. On the average, these deviations do not exceed 20 percent and can be assumed to be quite acceptable (Table 7). Selection of the model of the neutral ionosphere also weakly affects electrical conductivity values (Table 1). It was of interest to find how the results

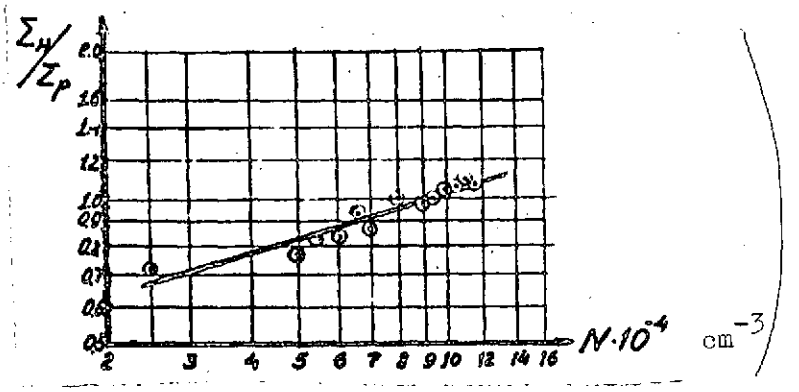

Fig. 8. Ratio Σ_H/Σ_P as function of maximum concentration of E-layer in the sunlit polar ionosphere

are affected by changes in the methods of calculating ν_{in}. For this purpose, conductivity was calculated from 80 N(h)-profiles, where ν_{in} was calculated by the formula

$$\nu_{in} \simeq 4\cdot10^{9}\,\frac{N_n}{2{,}7\cdot10^{19}}\cdot\sqrt{\frac{T}{300}}. \quad /11/$$

The function $\Sigma_{H,P} =$ /15

$= f(N)$ calculated from these results have the same correlations as Fig. 7, but Σ_H was reduced 58 percent, and Σ_P by 48 percent. A. M. Lyatskaya /9/ calculated the conductivity of the sunlit polar cap from the results of ionic soundings at the station Bukhta Tikhaya. In her calculations she used the CIRA-1965 model of the neutral atmosphere, and she calculated ν_{in} by the formula

$$\nu_{in} = 2{,}6\cdot10^{-9}(N_n + N_i)M^{-1/2}, \quad /12/$$

where N_i is the number density of ions, and M is the molecular weight. It was found that the mean values of Σ_P are 30 percent smaller, and Σ_H -- 60 percent smaller than our results, although the correlations persist. All three functions are shown in Fig. 10, where the main result is denoted with a solid line, the conductivity for the altered ν_{in} is denoted with a dashed line, and the results of A. M. Lyatskaya are denoted with a dot-dashed line. Conductivity was calculated from the N(h)-

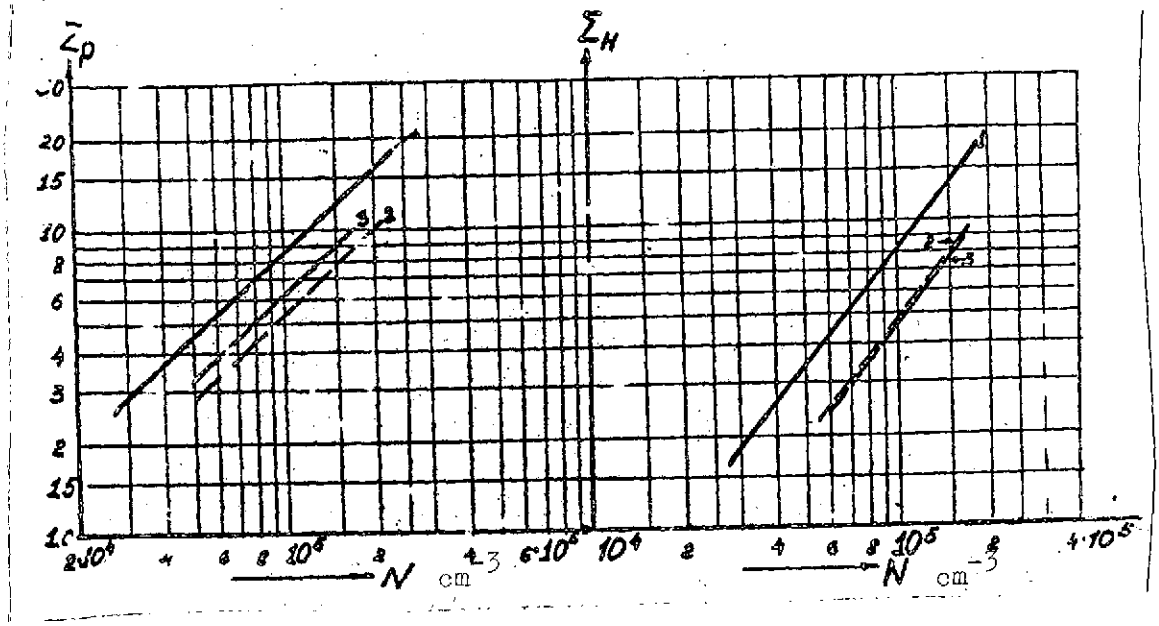

Fig. 9. Comparison of results of calculations of conductivities by three different methods

profiles No. 14, 15, and 16 from Table 7 in the paper [6]. Here the mean values of ν_{in} from data in the literature were used. Below we present a table in which the results are compared:

No.	From data in [6]			Results in present study		
	Σ_H	Σ_p	Σ_H/Σ_p	Σ_H	Σ_p	Σ_H/Σ_p
I4	34.5	I4.05	2.44	28	I2.2	2.3
I5	33.0	I6.2	2.I6	33	I5	2.2
I6	27.5	I5.5	I.77	24.6	I4.3	I.7

We see that the conductivities agree closely with each other. /16

Thus, a comparison of the different methods of calculation allow us to state that the possible deviations do not exceed 1.5-2 times. Here it is important to note that the ratios of the conductivities of the different ionospheric regions remain practically unchanged.

III. Schemes of Electrical Conductivity of the Polar Ionosphere

The above-established functions $\Sigma_{H,P} = f(N)$ made it possible to plot conductivity schemes, by using the hourly tables of critical frequencies of the E-layer for a network of ionospheric stations (Table 8). As an example, we present the schemes for January, June, and September 1960. Since in the constructions use was made of the median values of f_oE and f_BE_s, the resulting schemes characterize moderately active conditions. Two moments of world time were chosen -- 00:30 UT (nighttime on the American continent) and 17:00 (nighttime on the Asiatic continent).

In 1960, when ionograms of high-altitude stations in the USSR were being processed, a nighttime E-layer was differentiated. At the Canadian stations, this same layer was singled out as E_S with a group delay (type 2). In this case the values of f_BE_s were used in constructing the conductivity schemes.

As already stated, the critical frequencies of the E-layer and the conductivity tensor of the polar ionosphere depend simultaneously on the degree of solar illumination (zenith angle of the Sun) and on the geomagnetic activity. The first value is a function of the geographical coordinates, and the second -- /17
-- of the geomagnetic coordinates. The observed quantities reflect the total effect:

$$f_oE = F_1(\lambda, \varphi) + F_2(\Lambda, \Phi)$$

The inadequate number of ionospheric stations compels us to use all available hourly measurements. Here, we must separate F_1 and F_2 and represent the part associated with photoionization in geographical coordinates, and the second part associated with fluxes -- in geomagnetic coordinates.

The critical frequency of the E-layer as a function of the zenith angle of the Sun is quite accurately expressed by the

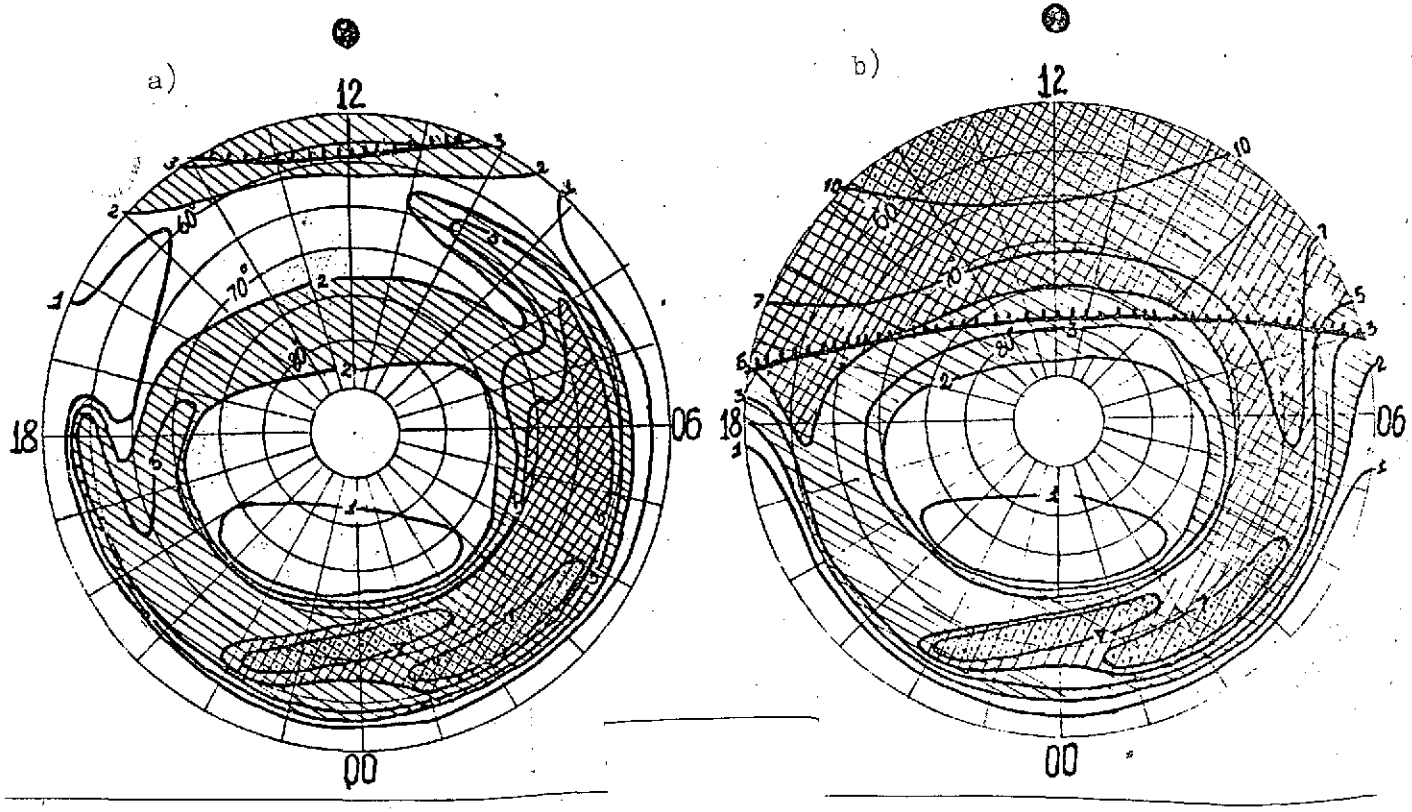

Fig. 10. Schemes of distribution of integrated conductivities in polar ionosphere, in Junary 1960: a) Σ_P at 05:00 UT b) Σ_P at 17:00 UT

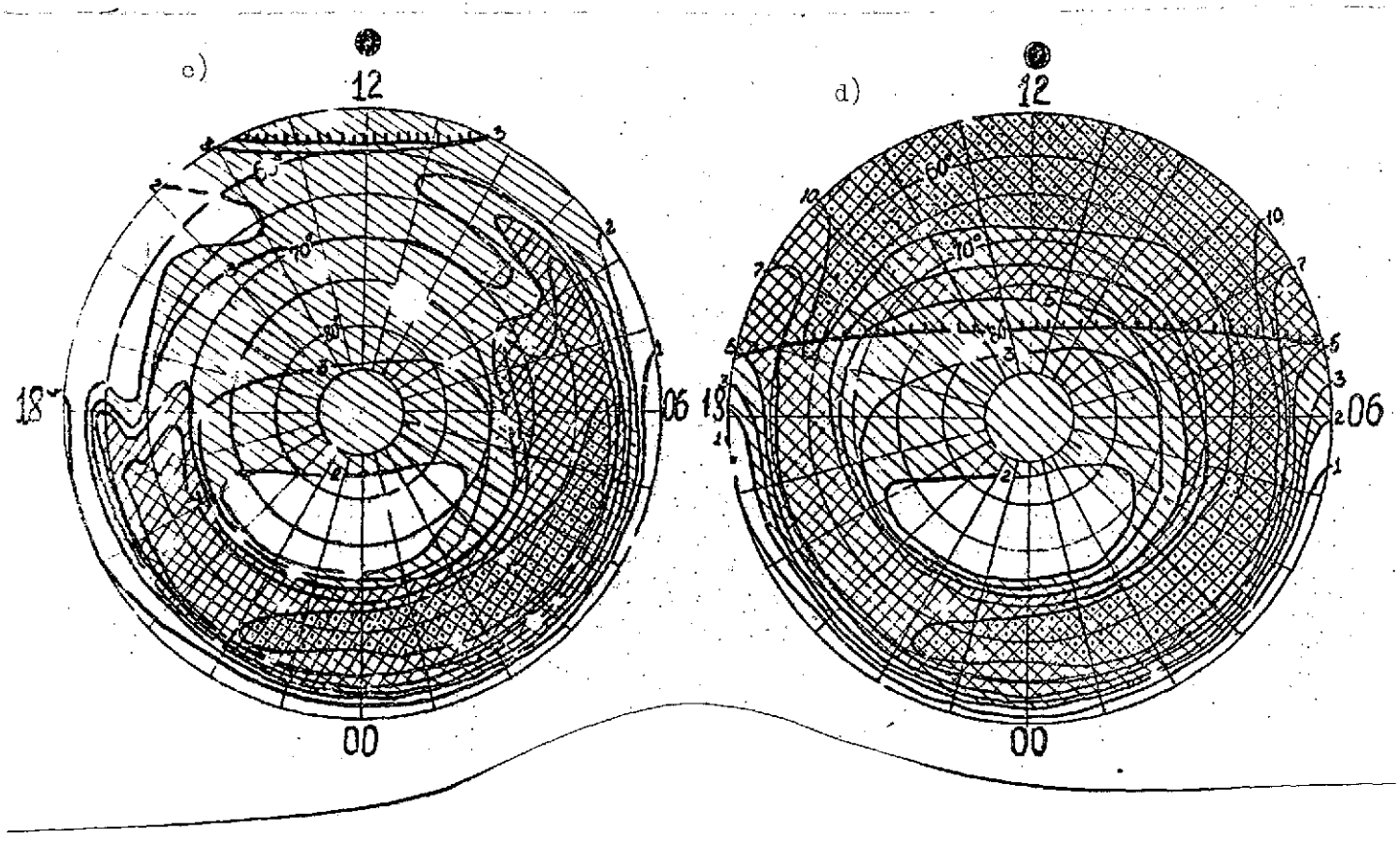

Fig. 10. Schemes of distribution of integrated conductivities in polar ionosphere, in January 1960: c) Σ_H at 05:00 UT d) Σ_H at 17:00 UT

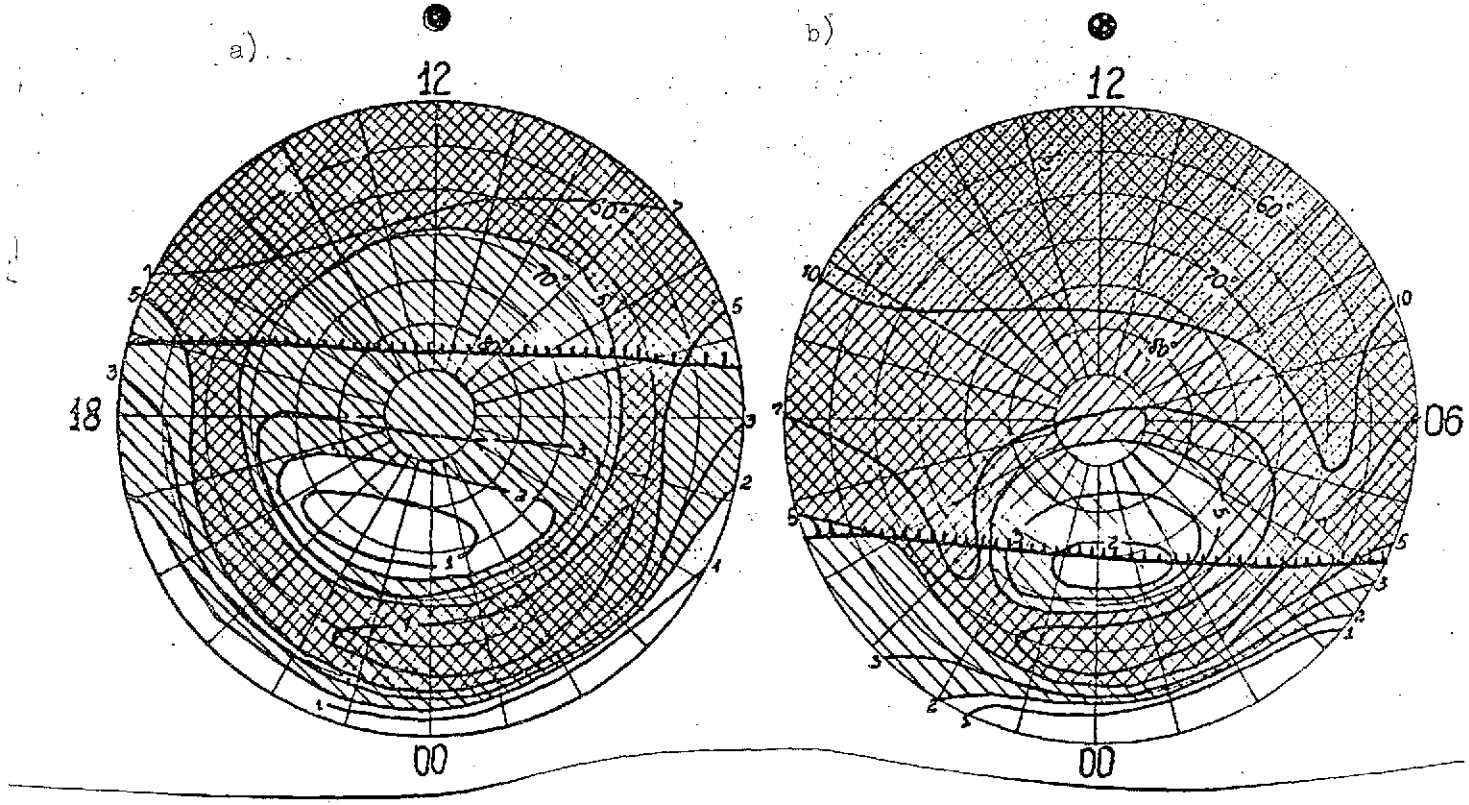

Fig. 11. Schemes of distribution of integrated conductivities in polar ionosphere in September 1960: a) Σ_P at 05:00 UT b) Σ_P at 17:00 UT

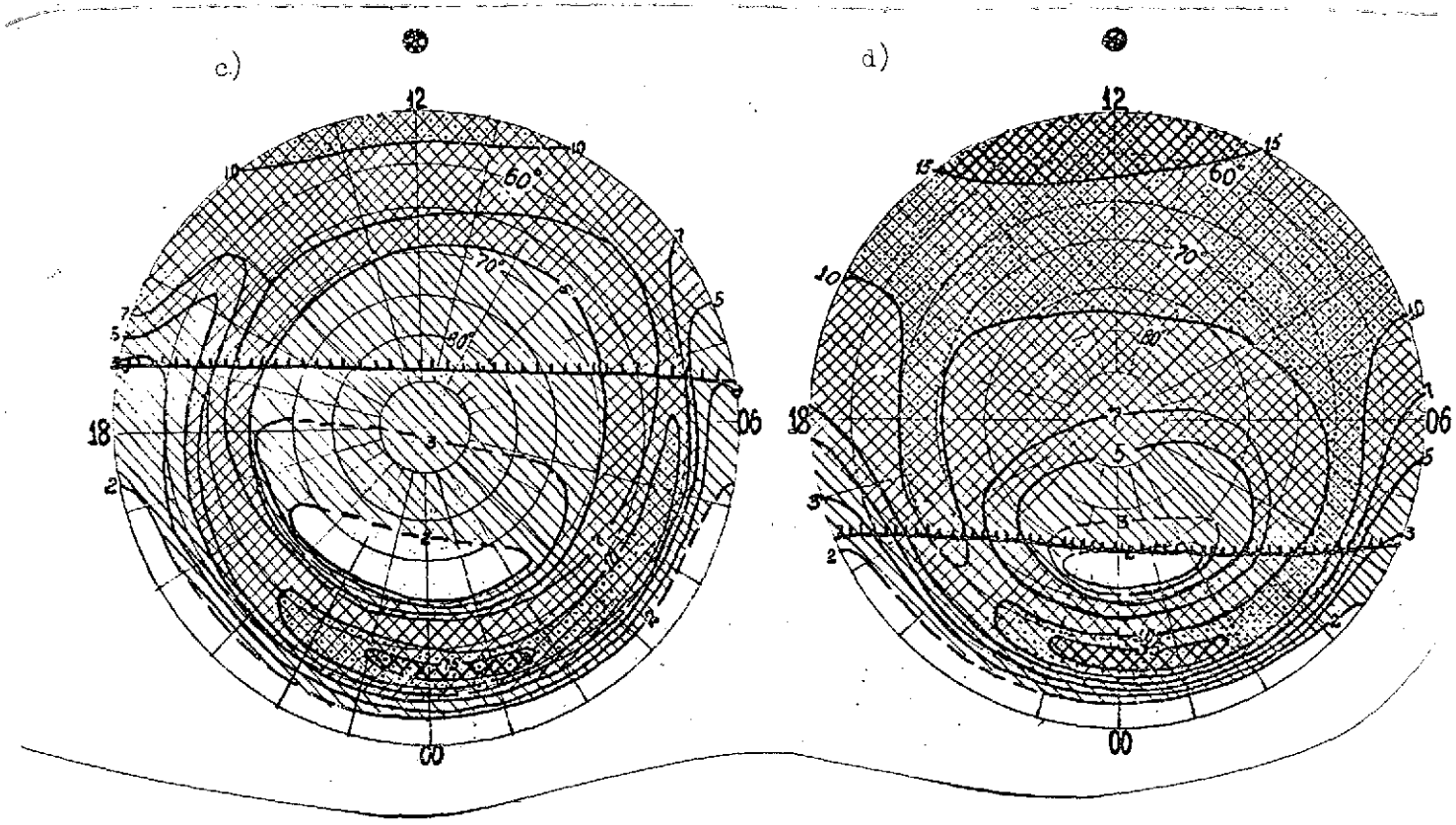

Fig. 11. Schemes of distribution of integrated conductivities in polar ionosphere in September 1960: c) Σ_H at 05:00 UT d) Σ_H at 17:00 UT

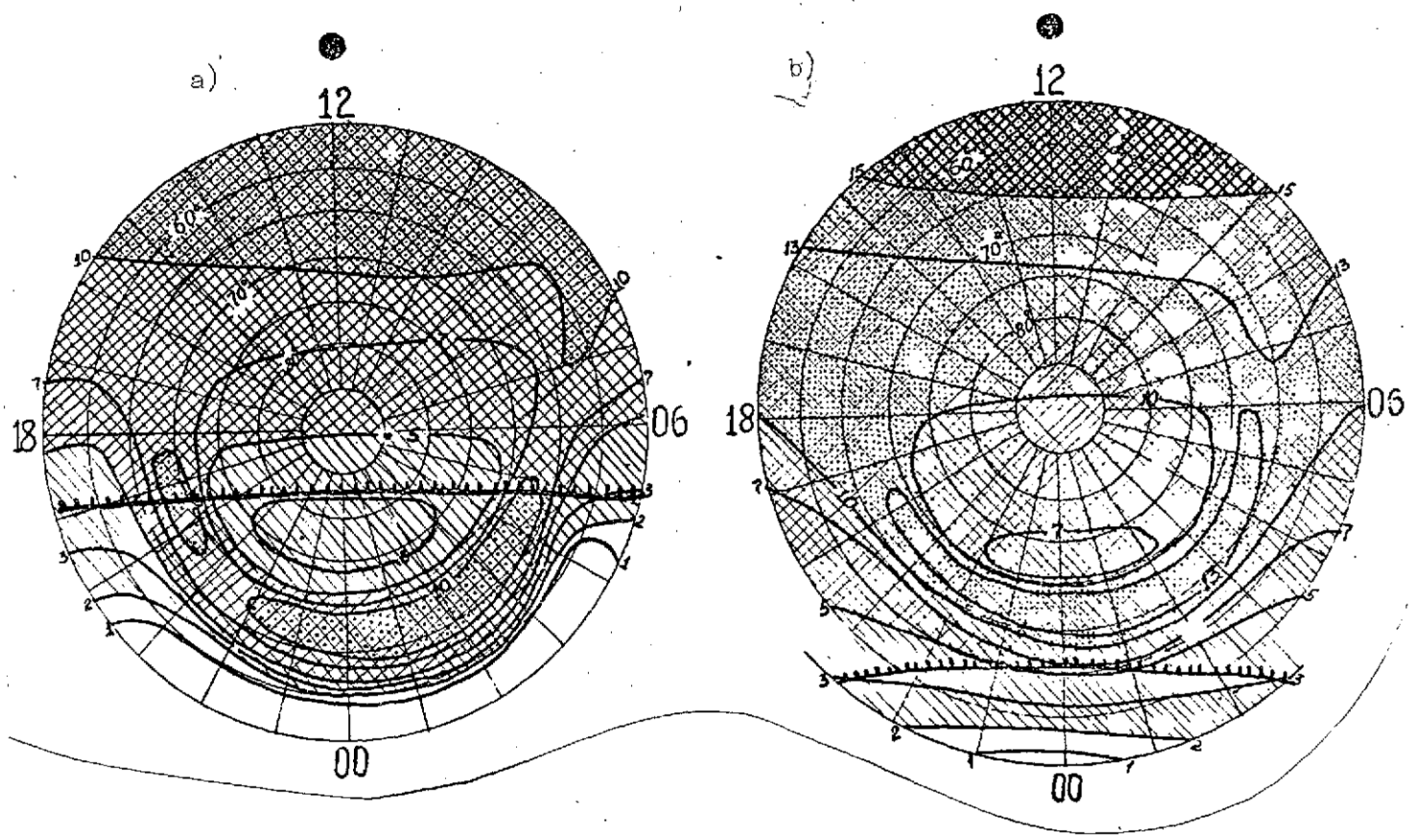

Fig. 12. Schemes of distribution of integrated conductivities in June 1960:
a) Σ_P at 05:00 UT b) Σ_P at 17:00 UT

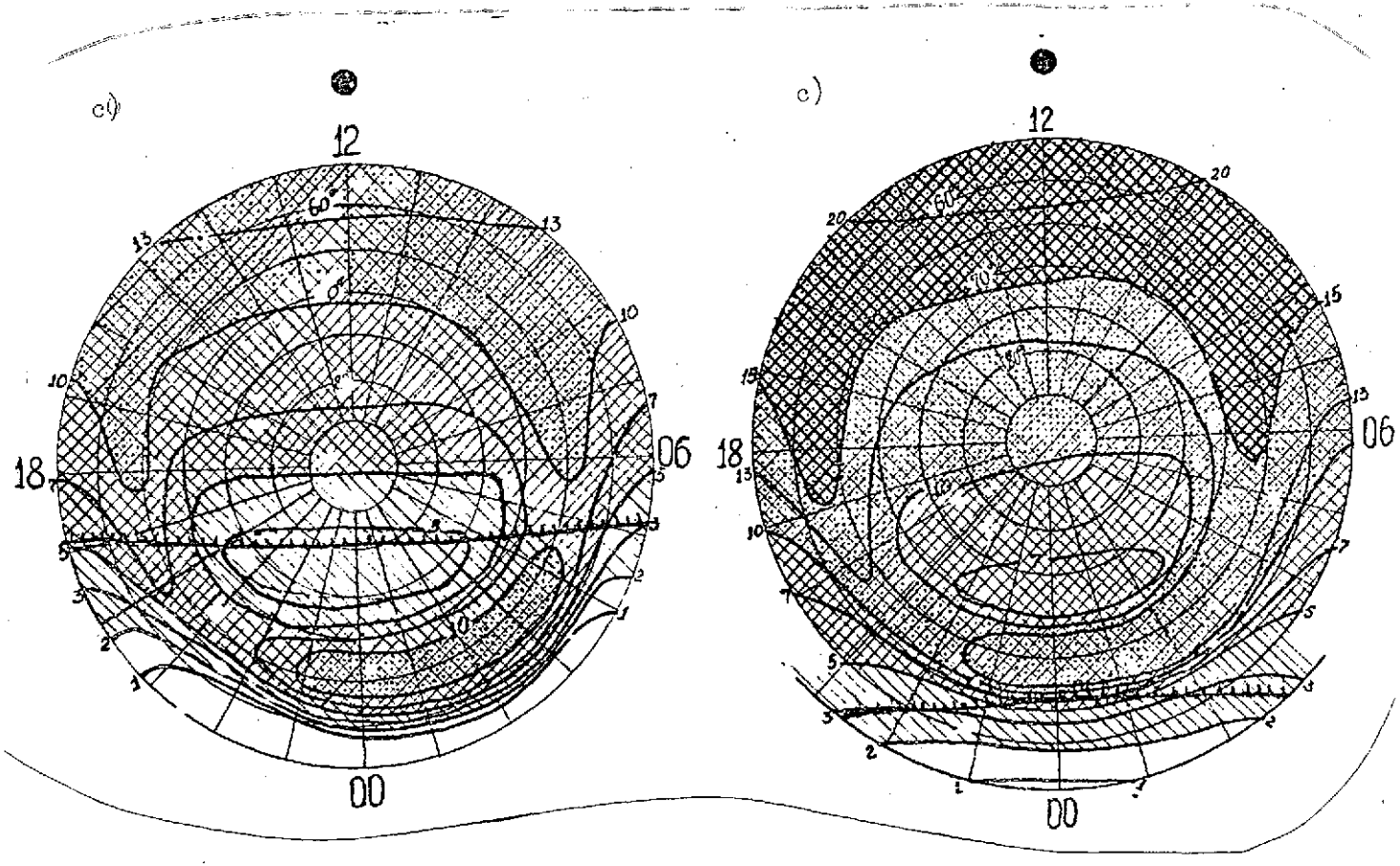

Fig. 12. Schemes of distribution of integrated conductivities in June 1960:
c) Σ_H at 05:00 UT d) Σ_H at 17:00 UT

cosine law, and on this basis monthly forecast maps of the critical frequency of the E-layer are constructed. This made it possible, by subtracting from the observed critical frequencies the forecast frequency, to determine the anomalous part associated with geomagnetic activity.

The schemes were constructed as follows:

1. The boundary of the illumination of the ionosphere at the level of the E-layer in local time was determined for each station.

2. The values of Σ_H and Σ_P were determined for the dark ionosphere from the plot $\Sigma_{H,P} = f(N)$ in Fig. 3, and these values were entered on the corresponding schemes in geomagnetic coordinates.

3. The values of Σ_H and Σ_P were determined from the plot $\Sigma_{H,P} = f(N)$ in Fig. 7 for the sunlit ionosphere.

4. The critical frequencies of the E-layer in the sunlit portion were compared with the forecast frequencies. When there was agreement, the conductivities were entered in the scheme in geographic coordinates. When there was disagreement, the conductivities obtained by the plot $\Sigma_{H,P} = f(N)$ (Fig. 7) from forecast data were entered in geographical coordinates, and the difference between the conductivities obtained based on observations and forecast data were plotted in geomagnetic coordinates. /18

5. The schemes plotted in geographical and geomagnetic coordinates were placed one over the other for a specific world time and the conductivities were added, after which the equal-conductivity lines were drawn.

Let us proceed to describing the schemes that enable us to answer an important question: what is the nature of the

coupling of the region of increased conductivity due to corpuscular fluxes with the ionosphere illuminated by the Sun?

In January, the boundary of illumination lies at + 60° Greenwich Mean Latitude. This means that the entire polar cap north of 60° is in darkness (Fig. 10). In the auroral latitude (60-70°) a well-defined zone of increased conductivity with maximum Σ_H = 13 mho and Σ_P = 8.0 mho becomes evident. It is a ring broken in the post-meridian hours and not in contact with the sunlit ionosphere. Here the conductivity maximum is shifted toward the early morning hours. On the south, on the nighttime side the ring is encircled by the nighttime middle-latitude ionosphere with $\Sigma_{H,P} < 1$, and on the north lies the polar cap with $\Sigma_{H,P} \leqslant 1$. As we can see, the conductivity of the auroral zone exceeds the conductivity of the surrounding ionosphere by more than one order of magnitude. At the latitudes of the daytime dip a small rise in conductivity can be distinguished: $\Sigma_P \approx 2$ mho and $\Sigma_H \approx 3$ mho.

In the Euro-Asiatic sector (17:00 UT) the distribution of electrical conductivity was substantially different. The terminator was at noon at +82° geomagnetic latitude, and during the daytime hours most of the polar cap was sunlit. The auroral region of increased conductivity, having during the nighttime hours the same structure as in the American sector, merged in the evening and morning hours with the sunlit region of increased conductivity. The region of the daytime dip was masked by the conductivity of the sunlit ionosphere. Thus, the schemes of ionospheric conductivity differed in that in the American sector the auroral zone of increased conductivity was a broken circle, surrounded on all sides by much lower conductivity, while in the Asiatic sector the ends of the conductive auroral zone merged with the sunlit ionosphere. /19

At equinox (September 1960) at 05:00 UT (Fig. 11), the pattern of the distribution of conductivity quite precisely

reproduced the distribution for the Asiatic sector in January. At 17:00 UT, the line of sunlit region was shifted to 75° geomagnetic latitude on the nighttime side. The sunlit ionosphere was shifted even further into the auroral zone of increased conductivity. In the polar cap there remained only a small minimum ($\Sigma_P \approx$ 2-3 mho). The conductivity of the auroral zone exceeded by two to three times the values in the polar cap. On the nighttime side, the auroral zone as before was confined by the poorly conductive nighttime middle-latitudinal ionosphere.

In June (Fig. 12), the pattern of distribution of $\Sigma_{H,P}$ for the American sector was close to that just described. In the Asiatic sector the terminator was shifted to 60° geomagnetic latitude. The entire region delimited by this parallel was sunlit. Since the corpuscular ionization was comparable with the solar, the auroral zone of increased conductivity appeared /20 in this case as well, but conductivity within it did not differ by more than 2-3 times from that of the surrounding ionosphere.

Thus, in examining the conditions for the formation of the electrojet in the auroral zone, one must bear in mind that it depends not only on the geomagnetic activity, but also on the geographic position of this region.

Conclusions

1. Based on rocket measurements and ground-based ionospheric soundings, the integrated Hall and Pedersen conductivities were obtained as functions of the critical frequency of the E-layer.

2. A study was made of the integrated conductivities as a function of magnetic activity.

3. For different seasons, interrelationships of two types of conductivity were established: 1) conductivity caused by photoionization, and 2) conductivity caused by the precipitating of energetic particles.

The authors are grateful to T. N. Soboleva, A. N. Sukhodol'skaya, A. M. Lyatskaya, and N. A. Zabolotnaya for assistance in this investigation.

REFERENCES

1. Kim, N. Y., and Kim, J. S., J. Atm. Terr. Phys. 25, 481 (1963).
2. Bostrom, R., J. Geophys. Res. 69, 4983 (1969).
3. McDiarmid, D. R., and McNamara, A. G., Canad. J. Phys. 47, 1271 (1969).
4. Rees, M. H., and Walker, J. C. G., Ann. Geophys. 24, 193 (1968).
5. Foppl, H., Haerendel, G., Haser, L., and Lust, R., J. Geoph. Res. 73, 21 (1968).
6. Kist, R., and Spenner, K., Zeitschrift fur Geophysie 36, 421 /year not given/.
7. Zaytsev, A. N., "Analysis of Variations of the Magnetic Field in High Latitudes," Dissertation in Defense of the Degree of Candidate of Physico-Mathematical Sciences, Moscow.
8. Soboleva, T. N., "Global model of integrated transverse conductivity of the ionosphere," Preprint Deposited No. 3504-71, Moscow, 1971.
9. Lyatskaya, A. N., Astakhov, P. G., and Bryunelli, V. Ye., "Conductivity of high-latitude ionosphere during quiet and active periods," Report presented at the International Association of Geomagnetism and Aeronomy, 1970.
10. Jacchia, /first initial not given/, "New static models of the thermosphere and exosphere with empirical temperature profiles," Research in Space Science, SAO Special Report No. 313, May 6, 1970, Cambridge, Massachusetts.
11. Ginzburg, V. L., Rasprodeleniye elektromagnitnykh voln v plazme /Distribution of electromagnetic waves in plasma/, Nauka Press, Moscow, 1967.
12. Chapman, S., Nuovo Cimento Suppl. 4, 1385 (1956).
13. Kamigama, H., and Sato, T., The Science Reports of the Tohoku Univ., 1957, Series 5, Geophysics, Vol. 9, p. 55.
14. Stubbe, P., Journal Atm. Terrestr. Phys. 30, 1965 (1968).
15. Whitten, R. K., and Poppov, I. J., Fizika nizhney ionosfery /Physics of the Lower Ionosphere/, Moscow, 1968.